Heliyon 10 (2024) e38258

Contents lists available at ScienceDirect

Heliyon

journal homepage: www.cell.com/heliyon

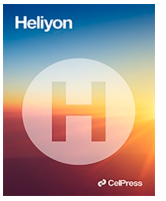

Research article

Role for NLRP3 inflammasome-mediated, Caspase1-dependent response in glaucomatous trabecular meshwork cell death and regulation of aqueous humor outflow

Xiaomei Feng, Zhao Chen, Wenjun Cheng, Changgeng Liu, Qian Liu *

Zhengzhou University People's Hospital, Henan Provincial People's Hospital, Henan Eye Hospital, Henan Eye Institute, Zhengzhou, China

ARTICLE INFO

Keywords:
Pyroptosis
NLRP3
ROS
Glaucoma
Human trabecular meshwork cell

ABSTRACT

Purpose: Acute ocular hypertension (AOH) is the defining feature of acute glaucoma. The mechanical stress and excessive production of reactive oxygen species (ROS) during episodes can directly or indirectly damage the trabecular meshwork (TM). Despite its significance, a clear understanding of its pathogenesis and an effective therapeutic target remain lacking in acute glaucoma. In the present study, we explored the potential molecular mechanisms underlying TM cell death following oxidative damage and AOH. The use of NAC/VX-765 as a potential pharmaceutical intervention for reducing intraocular pressure (IOP) was discussed.

Methods: The levels of NLRP3 and caspase-1 were compared between normal and glaucomatous TM samples. An in vitro oxidative damage model and an AOH rat model were used to investigate the potential molecular mechanism behind TM cell death. The ROS scavenger N-acetyl-L-cysteine (NAC) and caspase-1 inhibitor VX-765 were used to counteract TM damage.

Results: Elevated levels of NLRP3 and caspase-1 were observed in patients with acute glaucoma. H_2O_2 exposure decreased the viability of human trabecular meshwork (HTM) cells and increased intracellular ROS levels. Both Gene and protein expressions of NLRP3, caspase-1, GSDMD-N, and IL-1β were notably upregulated in H_2O_2-induced HTM cells and the rodent AOH model. Both NAC and VX-765 demonstrated protective effects against TM injury by inhibiting pyroptosis. The IOP-lowering effects of NAC and VX-765 persisted for 7 days.

Conclusions: Our findings indicate that the classical pyroptosis pathway, NLRP3/caspase-1/IL-1β, plays a key role in acute glaucomatous TM injury. Targeting pyroptosis provides novel therapeutic avenues for treating AOH-induced irreversible TM injury. This provides not only a promising therapeutic target for glaucoma but also introduces a new approach to intervention.

1. Introduction

Glaucoma is a leading cause of irreversible vision loss worldwide [1]. Sustained elevated intraocular pressure (IOP) is one of the most significant risk factors for the development of glaucoma. Elevated IOP is typically a result of increased aqueous humor drainage resistance [2]. Despite the existence of various therapeutic avenues, controlling intraocular pressure remains the predominant treatment approach for glaucoma at present [3].

* Corresponding author. Zhengzhou University People's Hospital, Henan Provincial People's Hospital, Henan Eye Hospital, No. 7 Weiwu Road, Zhengzhou, Henan, 450003, China.
E-mail address: 439640104@qq.com (Q. Liu).

https://doi.org/10.1016/j.heliyon.2024.e38258
Received 2 January 2024; Received in revised form 19 September 2024; Accepted 20 September 2024
Available online 25 September 2024

The trabecular meshwork (TM) serves as the primary outflow pathway for aqueous humor drainage, and the specialized cribriform structure of TM maintains its function [4]. Throughout an individual's life, TM cells undergo a gradual decline [5]. Studies have demonstrated a steeper decline of TM cells among glaucoma patients than in age-matched controls [6–8]. This compromised TM cellularity, in tandem with the functional decline of the meshwork's structure, is postulated to contribute to the dysfunction of the outflow pathway in glaucoma [9,10].

Pyroptosis is a novel form of programmed cell death that is closely associated with inflammatory response. Distinct from other types of programmed cell death, such as apoptosis, autophagy, and ferroptosis, in both morphology and mechanism, pyroptosis is characterized by plasma membrane disruption, which subsequently results in cell swelling and lytic cell death [11]. The NLRP3 inflammasome is a multiprotein complex, whose activation is crucial in driving pyroptosis. NLRP3 activates pro-caspase-1, converting it into the executioner caspase-1 [12]. This in turn catalyzes the cleavage of pre-IL-1β and pre-IL-18 through the classical inflammasome signaling pathway. Previous studies suggested that endogenous injury can promote the production of reactive oxygen species (ROS), leading to the activation of NLRP3/caspase-1-dependent pyroptosis [13].

Recent studies suggest that pyroptosis occurs in primary eye structures, including retinal ganglion cells (RGCs), Müller cells, astrocytes, microglia, endothelial cells, retinal epithelial cells, and TM cells [14–16]. Severe retinal hypoxia can diminish mitochondrial respiratory function, leading to mitochondria breakdown. This creates a vicious circle with hypoxia and accelerates the occurrence of pyroptosis [17,18]. Zheng et al. found that an increase in ROS leads to NLRP3 inflammasome activation in a murine dry eye model [19]. As an inflammatory disease, glaucoma sees an elevation of IOP that activates the NLRP3 inflammasome pathway in the glial cells of the optic nerve head (ONH), leading to the death of RGCs [18]. Li et al. provided evidence that $PM_{2.5}$ impacts TM tissues, contributing to the initiation and development of glaucoma [20]. However, the expression of key pyroptosis proteins in the TM and their role in glaucoma remain to be elucidated. Furthermore, the efficacy of ROS scavengers and pyroptosis inhibitors on TM in vivo has not yet been demonstrated.

In this study, we investigated the mechanism of NLRP3/caspase-1/IL-1β pyroptosis pathway activation in ROS-induced TM both in vitro and in an acute ocular hypertension (AOH) rodent model. We further explored the effectiveness of NAC/VX-765 in vitro and in vivo. Our findings suggest that pyroptosis participated in the development of ocular hypertension in glaucoma, highlighting the potential of NAC/VX-765 as a promising pharmaceutical intervention for reducing IOP.

2. Materials and methods

2.1. Ethics statements and consent to participate

(1) Statement of human rights: All procedures performed in studies involving human participants were following the ethical standards of the Clinical Research Ethics Committee of Henan Provincial People's Medical Ethics Committee and Zhengzhou University and with the 1964 Helsinki Declaration and its later amendments or comparable ethical standards (HNEEC-2023(41)). Informed consent was obtained from all participants and/or their guardians. (2) Statement on the welfare of animals: All experimental operations on animals by Henan Provincial People's Medical Ethics Committee and Zhengzhou University Animal Care and Ethics Committee (HNEECA-2023-05).

2.2. HTM samples preparation

The TM tissues were obtained by trabeculectomy from three patients diagnosed with primary open-angle glaucoma (POAG), including one 57-year-old female, one 57-year-old male, and one 75-year-old male. The preoperative intraocular pressure (IOP) values were 45.8 mmHg, 32.7 mmHg, and 26.5 mmHg, respectively. Additionally, three postmortem corneoscleral specimens were included, consisting of two males aged 50 and 67, and one 58-year-old female. The exclusion criteria of postmortem corneoscleral limbus specimens at the beginning of the study were any ocular disease history or general pathology associated. All surgeries were performed by a fellowship-trained glaucoma specialist with a minimum experience of 30 trabeculectomies [21–23]. Three TM surgical specimens and the postmortem corneoscleral specimens were fixed in 4 % paraformaldehyde (Biosharp, Hefei, China) [24]. The fragments of TM harvested during surgery were studied by immunofluorescence for the levels of NLRP3 and caspase-1.

2.3. HTM cell culture and treatment

The HTM cell lines were purchased from Shanghai Xuanya Biological Co., Ltd. (Shanghai, China), which were authenticated by short tandem repeat (STR) profiling. The third to sixth passages of the TM cells were used in the experiment. Cells were cultured at 37 °C with 5 % CO_2 in DMEM/F12 (D6570, Solarbio, Beijing, China) with 15 % fetal bovine serum (35-081-CV, Corning, NY, USA) and penicillin/streptomycin (32105, Mengbio, China) HTM cells were exposed to H_2O_2 (Tianjin, China) for 12 h to induce ROS injury, with medium serving as a control.

The ROS scavenger NAC (A9165, Sigma, USA) at a concentration of 10 mM or the caspase-1-selective inhibitor VX-765 (s2228, Selleck, USA) at a concentration of 100 μM were pre-treated for 2 h to provide protection before ROS injury by 200 μM H_2O_2 induced. All experiments were repeated three times.

2.4. Animals and groups

Male Sprague-Dawley (SD) rats weighing 200–250 g [25] were randomly assigned to the five groups. Animals were grouped as follows: (Group A-E): group A: control group, eyes that accepted no treatment; group B: AOH group, eyes that only underwent saline pressurization without any accompanying treatment; group C: negative control for drug groups, eyes that treated with 4 μL of phosphate-buffered saline (PBS) in the anterior chamber (AH) after saline pressurization; group D: therapeutic drug group 1, eyes that treated with 4 μL of NAC (20 mM) [26] in AH after saline pressurization; group E: Therapeutic drug group 2, eyes that treated with 4 μL of VX-765 (200 μM) [27] in AH after saline pressurization. The right eye of all animals is the experimental eye.

2.5. Animal model of acute ocular hypertension

To further validate the occurrence of pyroptosis in the TM tissue and elucidate the mechanism behind changes in IOP following acute ocular hypertension, a rat model of acute ocular hypertension was utilized.

The rats were anesthetized with 40 mg/kg of 1 % sodium pentobarbital (CAS:302-17-0, Macklin, China) via intraperitoneal injection, and their corneas were treated with 0.5 % proparacaine (SomnoSuite; Kent Scientific, Torrington, CT, USA) followed by 1 % tropicamide (SomnoSuite; USA) to dilate the pupils. A 30-gauge injection needle (BD, Franklin Lakes, USA) connected to a saline infusion reservoir was carefully inserted into the AH of the rat at the temporal corneosclera limbus and fixed and the AH pressure was gradually increased to 70 mmHg by adjusting saline set height; the pressure was monitored in real-time with a rebound tonometry (TonoLab; ICare, Espoo, Finland) for 120 min to ensure stability above this level [28,29]. The untreated contralateral eye was used as a blank control. Tobramycin ointment (Alcon, Fort Worth, Texas, USA) was applied to prevent infection in the treated eyes. After the end of the modeling, the intervention group further received 4 μL NAC (20 mM) in group D or 4 μL VX-765 (200 μM) in group E by AH injection. The group C was injected with 4 μL PBS in AH at the same time. No such treatment was conducted on the control group (group A). Eyes with lens or iris injury, or AH leakage were excluded from this study.

2.6. Cell viability test (CCK-8)

Cell viability was assessed using the CCK-8 assay (Dojindo, Kumamoto, Japan). HTM cells were seeded in a 96-well plate containing 5000 cells per well and were exposed to varying concentrations of H_2O_2 (0 μM, 100 μM, 200 μM,300 μM, and 400 μM) for 6 h,12 h, and 24 h.

After incubating with CCK-8 solution (1:10) at 37 °C for 2 h, the optical density (OD) was measured at a wavelength of 450 nm using a microplate reader (Molecular Device, Sunnyvale, CA, USA). NAC (10 mM) or VX-765 (100 μM) was applied to rescue experiments 2 h before exposure to 200 μM H_2O_2. The interference of the dissolving agent on the results was excluded.

2.7. Intracellular reactive oxygen species (ROS) and assays

The cytoplasmic ROS level was detected by measuring the oxidative conversion of cell-permeable dichlorodihydrofluorescein diacetate (DCFH-DA; S0033, Beyotime, China) to green fluorescent 2′,7′-dichlorofluorescein. The experimental operation was carried out according to the instructions. Cells were cultured in 6-well plates and incubated with diluted DCFH-DA (1 ml per well) at 37 °C for 20 min, followed by three washes with serum-free culture medium. Visualized the cells with fluorescence microscopy (ZEISS, Tokyo, Japan). Fluorescence signals were measured using ImageJ (Version 1.52a, NIH, USA) software and normalized to the control group for comparison. NAC(10 mM)rescue experiments were conducted as described above.

2.8. RNA isolation and reverse transcription-quantitative polymerase chain reaction (RT–qPCR)

HTM cells were collected after 12 h of H_2O_2 treatment, while TM tissues from rats were isolated 2 h post-treatment of AOH injury or drug injection. The TM tissues isolated from the rates eyes of the same experimental group were pooled [30]. Total RNA was extracted using TRIzol reagent (Ambion, Carlsbad, CA, USA) and its concentration was measured with a NanoDrop 2000 spectrophotometer (Thermo Scientific, Wilmington, DE, USA). First-strand cDNA was synthesized using the PrimeScript RT reagent kit (RR037A, Takara, Dalian, China). Samples were amplified using Power UpTM SYBR Green Master Mix (Thermo Fisher Scientific) in a 7500 Real-Time PCR System (Applied Biosystems, Thermo Fisher Scientific, MA, USA). Relative quantification was achieved by the comparative $2^{-\Delta\Delta CT}$ method. The primer sequences are listed below [20,31]:

Human NLRP3 Forward: 5′-GCACTTGCTGGACCATCCTC-3’,
Reverse: 5′-GTCCAGTGCACACGATCCAG-3’;
Human Caspase-1 Forward: 5′-AAGACCCGAGCTTTGATTGACTC-3’,
Reverse:5′-AAATCTCTGCCGACTTTTGTTTCC-3’;
Human IL-1β Forward: 5′-TATTACAGTGGCAATGAGG-3’
Reverse: 5′-ATGAAGGGAAAGAAGGTG-3’
Human β-actin Forward: 5′-CCCTGGACTTCGAGCAAGAG − 3’
Reverse: 5′-TCACACTTCATGATGGAGTTG-3’.
Rat: NLRP3 Forward: 5′-GTGGAGATCCTAGGTTTCTCTG-3’,
Reverse: 5′- CAGGATCTCATTCTCTTGGATC-3’;

Rat Caspase-1 Forward: 5′-GAGCTGATGTTGACCTCAGAG-3’
Reverse: 5′-CTGTCAGAAGTCTTGTGCTCTG-3’;
Rat IL-1β Forward: 5′-TGCTGTCTGACCCATGTGAG-3’,
Reverse: 5′-GTCGTTGCTTGTCTCTCCTTG-3’
Rat β-actin Forward: 5′-AGACCTTCAACACCCCAG-3’
Reverse: 5′-CACGATTTCCCTCTCAGC-3’.

2.9. Enzyme-linked immunosorbent assay (ELISA)

The protein level of IL-1β from cultured supernatants of HTM cells was measured using an IL-1β ELISA kit (RK00001, ABclonal Biotech Co., USA) according to the manufacturer’s instructions [32]. In brief, 100 μL of standard or sample was added to the corresponding wells of the microplate, wells were closed with plate sealing membrane, and the plates were incubated for 2 h at 37 °C. The solution was discarded and washed three times with 1× wash buffer. The biotin conjugate antibody working solution (100 μL/well) was added to each well and then incubated at 37 °C for 1 h. Next, the solution was discarded, washed three times, and streptavidin-HRP working solution (100 μL/well) was added to each well, and incubated at 37 °C for 30 min. The solution was discarded and the washing three times, and TMB substrate (100 μL/well) was added. The plates were incubated for 20 min at 37 °C in the dark. Termination solution (50 μL/well) was added and immediately placed into a microplate reader to determine the OD at 450 nm with a microplate reader (Molecular Device, Sunnyvale). IL-1β levels were determined from the standard curve.

2.10. Western blot analysis and antibodies

Total protein was extracted by RIPA lysate (P0013K, Beyotime) containing 1 % cocktail (GRF101, EpiZyme, China), and the protein concentration was determined by the BCA electrophoresed on a 10 % SDS-PAGE (PG112, EpiZyme) and transferred onto PVDF membranes (0.45 μm, IPVH00010, Millipore, USA). After blocking in 5 % skim milk for 2 h, membranes were incubated overnight at 4 °C with primary antibodies. Then membranes were incubated with a second antibody-HRP conjugate (abs20002, absin, China) for 2 h at room temperature and visualized with Chemiluminescent detection reagent (WBKLS0500, Millipore, USA). Results were analyzed using ImageJ (Version 1.52a, NIH, USA) software and normalized to GAPDH. The primary antibodies are listed below: anti-NLRP3 (1:1000, CAT#19771-1-AP, proteintech, Chicago, USA) [33]; anti-Caspase-1(1: 1000, CAT#22915-1-AP, proteintech Chicago, USA) [33]; anti-GSDMD-N (1:1000, CAT#ab215203, Abcam, Boston, MA, USA) [20]; anti-GAPDH (1:10000, CAT#ab181602, Abcam, Boston, MA, USA).

2.11. Cellular immunofluorescence

HTM cells were fixed in 4 % paraformaldehyde (Biosharp, China) for 30 min, washed with PBS three times, then permeabilized with 0.1 % Triton X-100(T8200, Solarbio) in PBS for another 30 min and blocked with 5 % bovine serum albumin (BSA, Sigma, USA) for 1.5 h. Subsequently, cells were incubated overnight at 4 °C with primary antibodies against NLRP3(1:200, proteintech, Chicago, USA) [34] or caspase-1(1:100, proteintech, Chicago, USA) [33], followed by washing three times with PBS, secondary anti-rabbit IgG (H + L) Alexa Fluor®555 (1:200; A0453, Beyotime) were applied for 1 h at room temperature. Nuclei were stained with DAPI Staining Solution (P0131, Beyotime, China) in the dark for 5 min. PBS controls were incubated with PBS as the primary antibodies. Then, the samples were incubated with the corresponding secondary antibodies, under the same time and conditions as the experimental groups. The cells were visualized and captured using a Zeiss confocal microscope (Zeiss NLO780; Zeiss, Germany). Fluorescence intensity analysis using ImageJ(Version 1.52a, NIH, USA) software involved quantifying and normalizing the mean fluorescence intensity of experimental conditions to the control group [30].

2.12. Rat intraocular pressure (IOP) measurements

Rebound tonometry (TonoLab; ICare, Helsinki, Finland) [35] was used to measure the IOP [36]. Prior to the initiation of treatment, baseline IOP for each eye was obtained in rats. IOP was monitored at 1, 3, and 7 days after drug administration. Measurements were averages of three effective readings and were made at the same time of day and by the same observers [37].

2.13. Histology and immunostaining

Rats were killed by cervical-spinal transection after overdose anesthetized at 2 h post-modeling. Eyes were isolated from rats, and fixed with eye fixative solution (FAS, Servicebio, Wuhan, China) overnight. The surgically obtained TM tissues were immediately fixed in 4 % paraformaldehyde (G1101, Servicebio) overnight. For immunohistochemistry (IHC), the trimmed fixed tissue was dehydrated using various concentrations of ethanol, embedded in paraffin and cut into 4 μm-thick sections. The paraffin sections were placed in PBS (PH7.4) and washed 3 times on a decolorization shaker for deparaffinization. Next, sections were immersed in 3 % hydrogen peroxide solution for 25 min at room temperature in the dark and washed three times with PBS. After blocking with 3 % BSA for 30 min at room temperature. Sections were incubated with anti-NLRP3 (1:200, GB114320, Servicebio) and anti-Caspase-1 antibodies (1:500, GB11383, Servicebio) overnight at 4 °C and washed three times, followed by incubation with horseradish peroxidase (HRP)-conjugated secondary antibodies (1:200, GB23303, Servicebio) and washed three times. After DAB staining, the nuclei were counterstained

with hematoxylin. Following dehydration, sections were visualized under a bright-field panoramic scanning microscope (StrataFAXS Plus S, TissueGnostics, USA).

For fluorescence staining, the trimmed fixed tissue was dehydrated using sucrose solutions before being embedded in OCT (G6059-110 ML, Servicebio), and quickly frozen and cut into 8-10 μm-thick sections. Cryostat sections were incubated with anti-NLRP3(1:200, GB114320, Servicebio), and anti-caspase-1 antibodies (1:200, GB11383, Servicebio) followed by incubation with Cy3-labeled goat anti-rabbit IgG secondary antibodies (1:300, GB21303, Servicebio). PBS controls were incubated with PBS as the primary antibodies. Then, the samples were incubated with the corresponding secondary antibodies, under the same time and conditions as the experimental groups. Sections were visualized and photographed under a fluorescent microscope (NIKON ECLIPSE C1, Japan). Quantification was performed using ImageJ (Version 1.52a, NIH, USA) [30].

2.14. Statistical analysis

Statistical analysis was performed using GraphPad Prism version 9.0 software (GraphPad Software, USA). Results are presented as the mean ± standard error of the mean (SEM). Images were analyzed using the ImageJ software (Version 1.52a, NIH, USA).

The two-tailed Student's t-test was used to compare the differences between the groups, while one-way analysis of variance (ANOVA) was performed to investigate differences among multiple groups. $P < 0.05$ indicated significant differences.

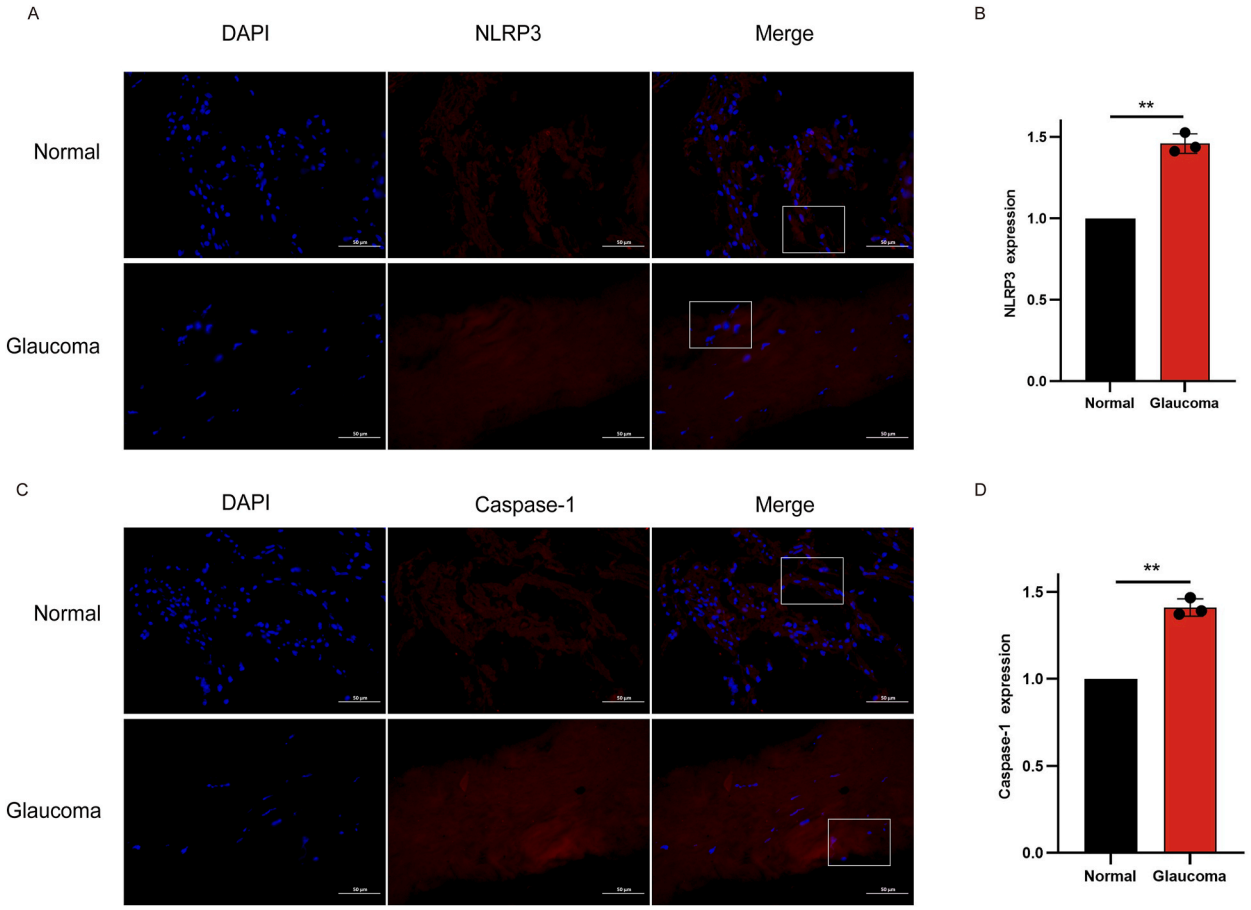

Fig. 1. Upregulation of NLRP3/caspase-1 in HTM tissues in patients with acute glaucoma. (1A and 1D) Immunofluorescence images showed a significant increase in the expression of NLRP3 and caspase-1 in the HTM tissues of glaucoma patients compared to the normal group. A region of a specific size was defined for quantification. (TM: trabecular meshwork, SC: Schlemm's canal, CB: ciliary body. Blue, nuclear staining with DAPI; red, NLRP3, caspase-1. Magnification, 20×. *$P < 0.05$, **$P < 0.01$ vs. normal. Data are presented as mean ± SEM. (For interpretation of the references to color in this figure legend, the reader is referred to the Web version of this article.)

3. Results

3.1. Pyroptosis is involved in the pathogenesis of glaucomatous TM injury

To determine whether pyroptosis plays a role in the pathogenesis of glaucomatous TM injury, we assessed the expression levels of NLRP3 and caspase-1 in TM tissues from patients with acute glaucoma and compared them to age-matched controls. The reduced nuclei count in glaucoma tissue compared to controls might be attributed to the limited region of TM tissues in trabeculectomy (Trab). However, the control specimens were the entire circumferential strip of TM. A standardized region was defined on the micrographs to minimize the effects on cell numbers. Fluorescence staining revealed a significant increase in both NLRP3 and Caspase-1 protein levels in TM tissues derived from glaucoma patients compared to TM tissues from healthy postmortem corneoscleral specimens (Fig. 1A–D). These results underscore the involvement of pyroptosis in glaucomatous TM damage.

3.2. H_2O_2 exposure triggered NLRP3/caspase-1/IL-1β/GSDMD-N pathway in HTM cells

To further investigate the role of pyroptosis in the pathogenesis of glaucoma, we established an in vitro model of H_2O_2-induced pyroptosis in TM cells [38,39]. Previous studies have shown that H_2O_2 exposure induces oxidative damage in cells, with the extent of damage from H_2O_2 being influenced by both the duration and concentration of exposure [40,41]. We exposed TM cells to varying H_2O_2 concentrations for 6 h, 12 h, and 24 h to determine the optimal concentration and exposure duration. The CCK-8 assay showed that HTM cell viability decreased in both a time- and concentration-dependent manner after H_2O_2 treatment. Notably, a statistically significant reduction in viability was observed after 12 h of exposure to 200 μM H_2O_2 (Fig. 2A).

Subsequent to H_2O_2 treatment at concentrations of 100 μM, 200 μM, and 300 μM, we measured the mRNA and protein expression of NLRP3, caspase-1, and IL-1β. Quantitative RT-PCR showed a significant increase in the mRNA levels of NLRP3 and caspase-1 following exposure to 200 μM and 300 μM H_2O_2 when compared to the controls (Fig. 2B). This increase was corroborated at the protein level by

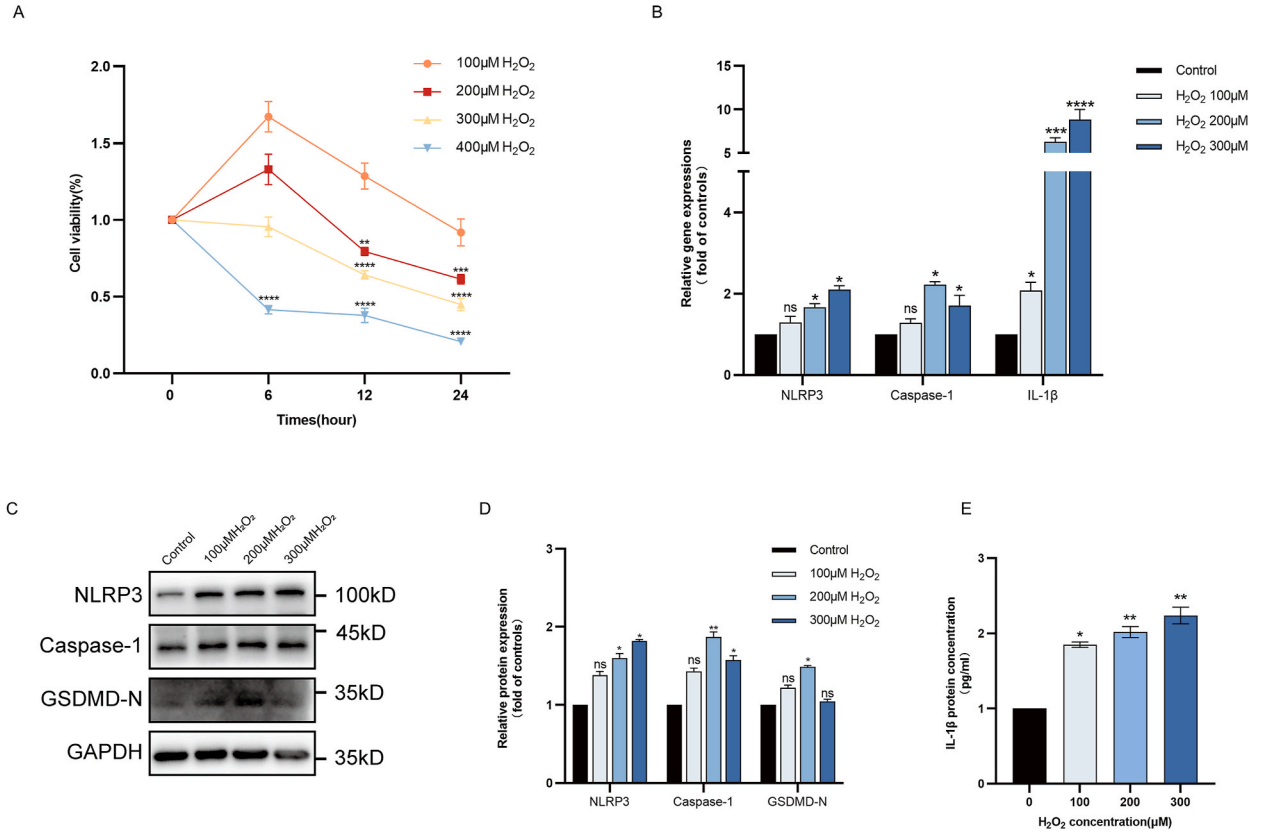

Fig. 2. Pyroptosis was increased in H_2O_2-treated HTM cells. (2A) CCK-8 assay results demonstrated that HTM cell growth was inhibited when exposed to 0 μM, 100 μM, 200 μM, 300 μM, and 400 μM H_2O_2 for 6 h, 12 h, and 24 h ($n = 5$). (2B) RT-qPCR results indicated that NLRP3, caspase-1 and IL-1β mRNA levels were increased with increasing concentrations of H_2O_2 ($n = 3$). (2C and 2D) Western blot analysis revealed an upregulation of NLRP3, caspase-1, and GSDMD-N protein levels with increasing H_2O_2 concentrations ($n = 3$). (2E) IL-1β protein levels were increased with increasing H_2O_2 concentrations, as demonstrated by ELISA ($n = 5$). (*$P < 0.05$, **$P < 0.01$ and ***$P < 0.001$ vs. control). Data are presented as mean ± SEM.

Western blot analysis, which confirmed elevated expressions of NLRP3 and caspase-1 in HTM cells exposed to 200 μM H_2O_2 (Fig. 2C and D). Additionally, the expression of GSDMD-N was consistent with the change of caspase-1 (Fig. 2C and D). The pro-inflammatory cytokine IL-1β in HTM cells also exhibited a concentration-dependent increase in response to H_2O_2 stimulation (Fig. 2E). Based on these results, a concentration of 200 μM H_2O_2 was utilized in the subsequent experiments.

3.3. NLRP3 was activated by H_2O_2 -induced increase in intracellular ROS level in HTM cells

ROS plays an important role in initiating and regulating the NLRP3 inflammasome, which in turn triggers caspase-1-dependent cell pyroptosis. To substantiate the activation of the ROS/NLRP3/caspase-1 pathway in HTM cells, we measured the intracellular ROS level post-treatment with 200 μM H_2O_2 using a fluorescent probe. Our results show that, compared to the control, the ROS level in the treated HTM cells elevated significantly, exhibiting an approximately four-fold increase after 12 h of 200 μM H_2O_2 exposure (Fig. 3A). In line with this elevation, immunofluorescence staining illustrated a marked increase in the levels of NLRP3 and caspase-1 in HTM cells after exposure to 200 μM H_2O_2 (Fig. 3B and C). This further supports the notion that increased intracellular ROS is essential for the activation of NLRP3/caspase1-dependent pyroptosis in HTM cells.

3.4. NAC or VX-765 effectively inhibits NLRP3/caspase-1/IL-1β/GSDMD-N expression in HTM cells in vitro

To further evaluate the impact of the classical pyroptosis pathway on TM cell damage and to identify potential therapeutic targets, we carried out experiments on HTM cells using the ROS scavenger N-acetylcysteine (NAC) and selective caspase-1 inhibitor VX-765. Before inducing ROS damage, cells were pretreated for 2 h with either NAC at a concentration of 10 mM or VX-765 at a concentration of 100 μM. Results show that pretreatment with either NAC or VX-765 significantly increased HTM cell viability (Fig. 4A), while also reducing intracellular ROS concentrations (Fig. 4B). Further, the pyroptotic activity was also significantly suppressed after treatment with these agents. This was corroborated by a significant reduction in the expression levels of NLRP3, caspase-1, and GSDMD-N

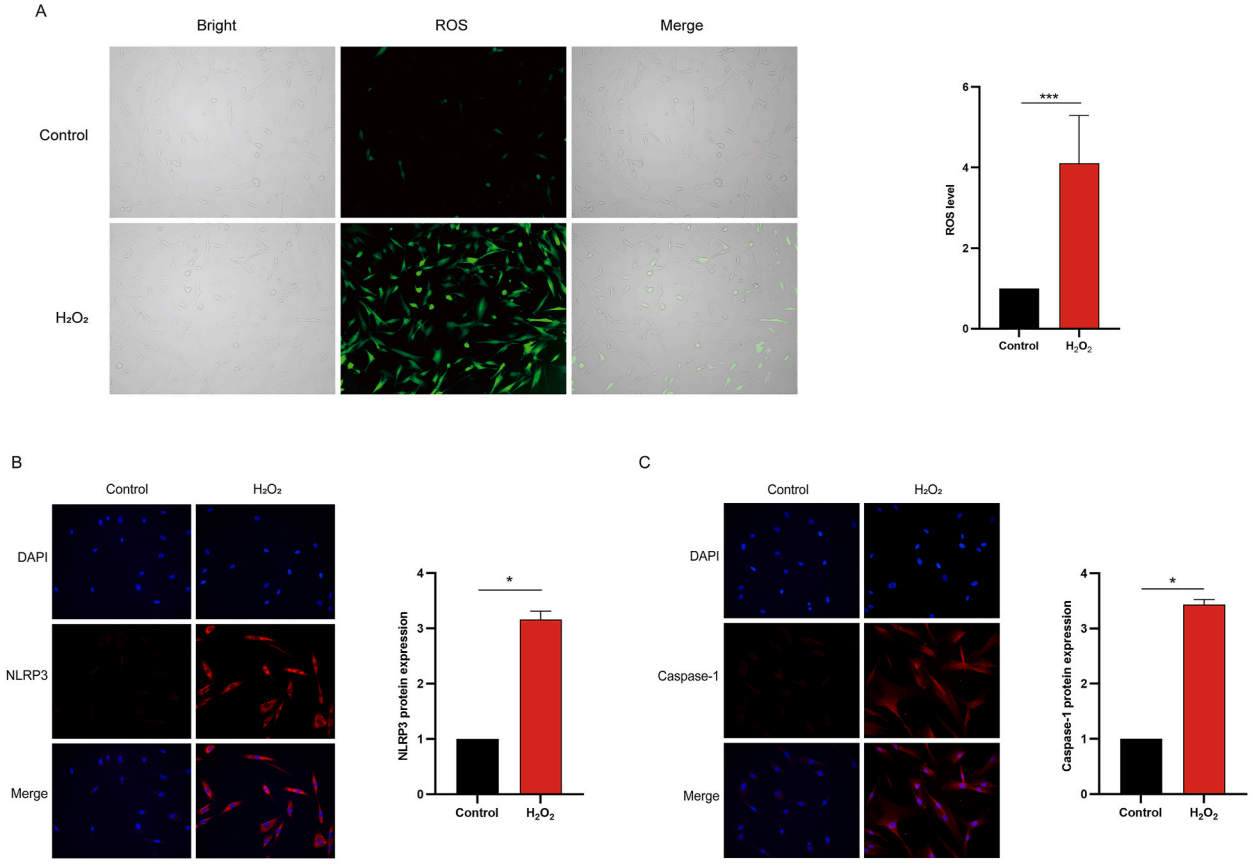

Fig. 3. ROS and immunocytofluorescence staining images of HTM cells. (3A) A significant increase in ROS level was observed in HTM cells after being treated with 200 μM of H_2O_2 ($n = 3$). (3B and 3C) NLRP3 and caspase-1 levels were significantly increased in HTM cells treated with 200 μM H_2O_2, and immunocytofluorescence analysis was performed. Blue, nuclear staining with DAPI; red, immunocytofluorescence staining ($n = 3$). Magnification, 20×. *$P < 0.05$, ***$P < 0.001$ vs. control) Data are presented as mean ± SEM. (For interpretation of the references to color in this figure legend, the reader is referred to the Web version of this article.)

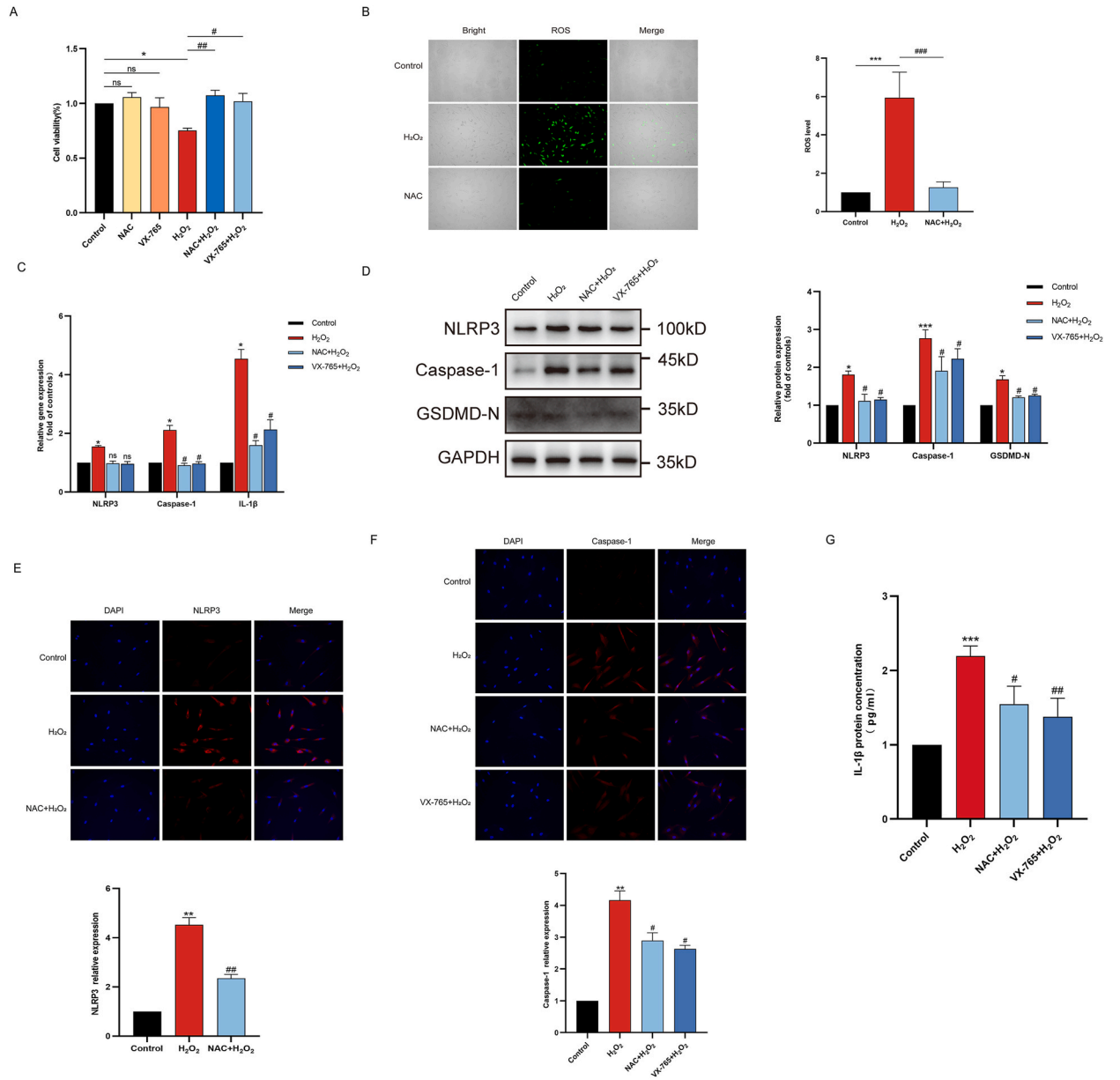

Fig. 4. ROS scavenger and caspase-1 inhibitor intervention on H_2O_2-induced toxicity and reduced pyroptosis in HTM cells in vitro. (4A) ROS scavenger NAC and VX-765 pretreated for 2 h improved HTM cell viability in cells exposed to 200 μM H_2O_2 for 12 h ($n = 3$). (4B) The fluorescence intensity reflecting ROS levels was significantly decreased in HTM cells treated with NAC. In each panel, the bright field, fluorescence, and merged image of fluorescence and bright field are arranged from left to right ($n = 3$). (4C) RT-qPCR analysis revealed a downregulation of NLRP3, caspase-1, and IL-1β after intervention with NAC and VX-765($n = 3$). (4D and 4G) Pyroptosis-related protein expressions of NLRP3, caspase-1, GSDMD, and IL-1β were found to be significantly reduced by Western blot and ELISA ($n = 5$). (4E and 4F) Immunofluorescence examination confirmed the NAC and VX-765 treatment effectively inhibited the expression of NLRP3 and caspase-1 ($n = 3$). Blue, nuclear staining with DAPI; red, immunocytofluorescence staining. Magnification, 20×. $^{*}P < 0.05$, $^{**}P < 0.01$, $^{***}P < 0.001$vs. control. $^{\#}P < 0.05$, $^{\#\#}P < 0.01$, $^{\#\#\#}P < 0.001$ vs. H_2O_2. Data are presented as mean ± SEM. (For interpretation of the references to color in this figure legend, the reader is referred to the Web version of this article.)

(Fig. 4C–F). Importantly, the mRNA and protein levels of IL-1β, which functions downstream of caspase-1, exhibited a significant decrease in inhibitor-pretreated TM cells compared to those exposed to 200 μM H_2O_2 alone (Fig. 4G). These findings suggest that the use of ROS scavengers and caspase-1 inhibitors effectively protects TM cells from pyroptosis induced by oxidative stress.

3.5. Expression of NLRP3/caspase-1/IL-1β expression in the normal and acute ocular hypertension injury rats

To further verify the role of the classical pyroptosis pathway in glaucomatous TM damage, we developed a rat model of AOH. The AOH model was established by elevating the AH pressure using saline infusion. We then compared the expression levels of NLRP3, caspase-1, and IL-1β contents between control rats and AOH-injured rats. Quantitative RT–PCR was employed to measure the mRNA levels of NLRP3/caspase-1/IL-1β in rat TM tissues. Results showed a significant increase in the AOH group (group B) compared to the control group (group A) (Fig. 5A). Additionally, both IHC analysis and immunofluorescence revealed a significant increase in the expression of NLRP3 and caspase-1 in TM tissue following a 2-h perfusion at an AH pressure of 70 mmHg, in comparison to the control group (group A) (Fig. 5B and C).

3.6. In vivo, treatment with NAC or VX-765 protects TM tissues from pyroptosis

We further evaluated the protective efficacy of NAC and VX-765 on TM tissue in vivo to assess their therapeutic potential. Post-inducing AOH, rats were administered either NAC or VX-765 through AH injection. For the negative control group, PBS was used. Animals were sacrificed 2 h post-perfusion and gene expression of NLRP3/caspase-1 and the inflammatory marker IL-1β in the TM were analyzed. Results showed a significant reduction in their mRNA levels in NAC or VX-765 treated rats, compared to the negative control (group C) (Fig. 6A). Furthermore, protein levels of NLRP3 and caspase-1 were significantly inhibited in NAC/VX-765 treated groups (group D and group E) as confirmed by IHC analysis and immunofluorescence (Fig. 6B–D). This data emphasizes the efficacy of NAC and VX-765 in defending against AOH-induced pyroptosis in TM in vivo.

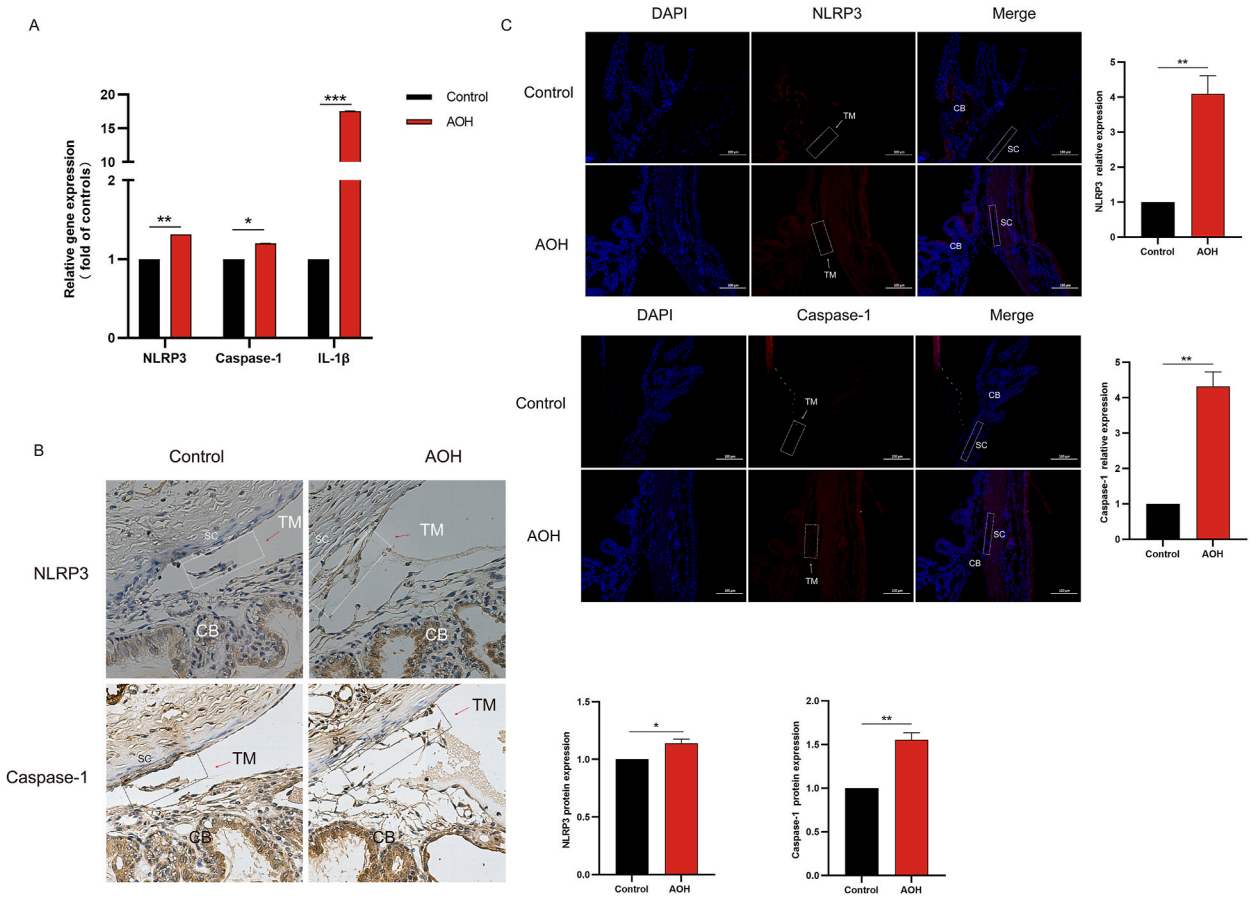

Fig. 5. The AOH-induced acute injury led to TM tissue pyroptosis. (5A) RT-qPCR detection of TM levels of NLRP3, caspase-1, and IL-1β (normalized to that of β-actin) in control and AOH-injured rats ($n \geq 3$). (5B, 5C) Representative photomicrographs of immunohistochemistry and immunofluorescence staining for NLRP3 and caspase-1 in TM tissue ($n \geq 3$). (TM: trabecular meshwork, SC: Schlemm's canal, CB: ciliary body. Magnification: 20×. $^{*}P < 0.05$, $^{**}P < 0.01$, $^{***}P < 0.001$vs. control). Data are presented as mean ± SEM.

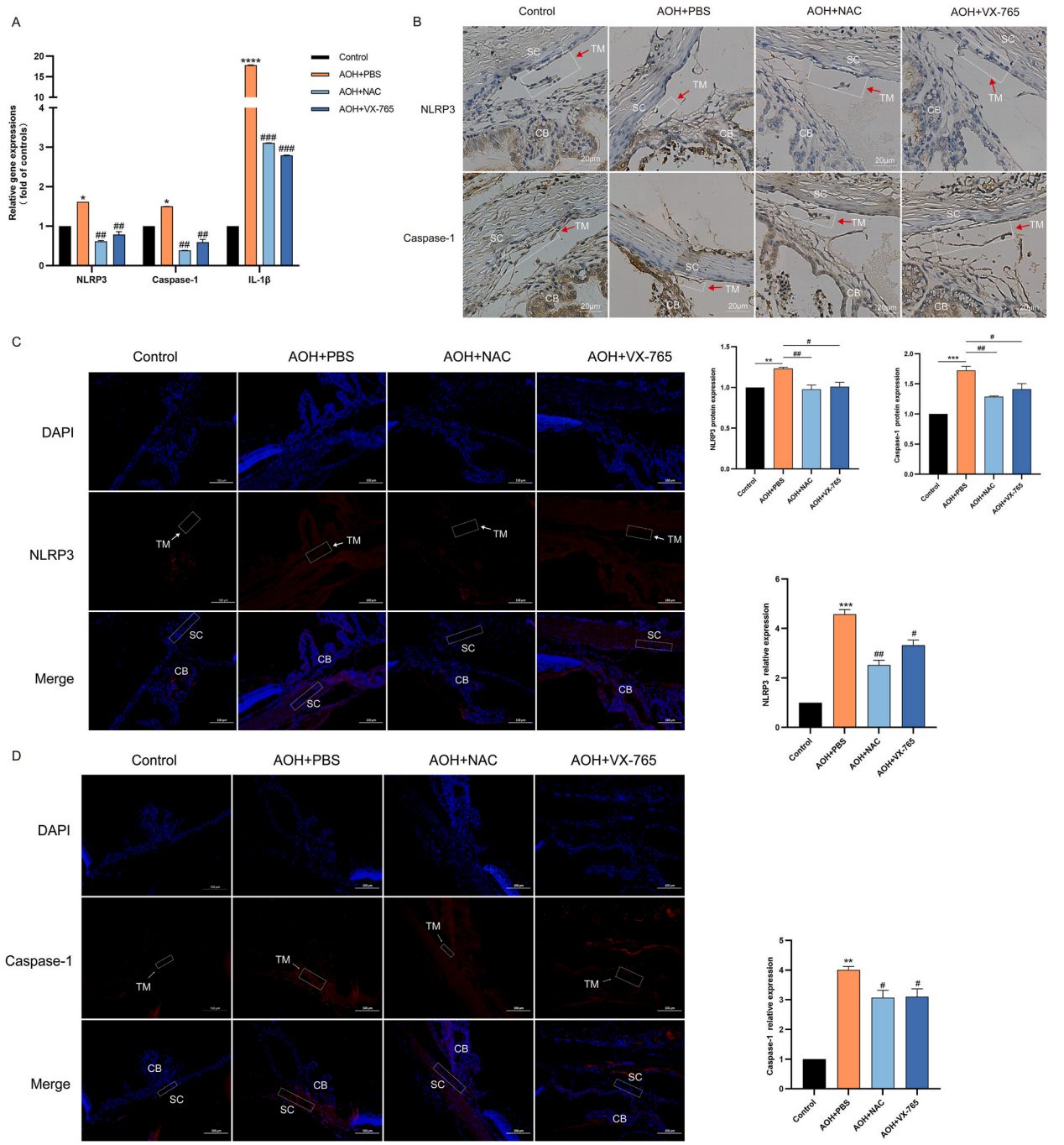

Fig. 6. NAC and VX-765 interventions on AOH-induced TM pyroptosis. (6A) The increased mRNA expression of NLRP3, caspase-1, and IL-1β induced by AOH was significantly inhibited on treatment with either NAC (20 mM) or VX-765 (200 μM). (6B-6D) Immunohistochemistry and immunofluorescence examination confirmed that NAC and VX-765 inhibited AOH-triggered NLRP3 and caspase-1 activation in TM ($n \geq 6$). Magnification, 20×. Blue, DAPI; red, NLRP3 (6C) or caspase-1 (6D) ($n \geq 6$). (TM: trabecular meshwork, SC: Schlemm's canal, CB: ciliary body. $^{*}P < 0.05$, $^{**}P < 0.01$ vs. control, $^{\#}P < 0.05$, $^{\#\#}P < 0.01$, $^{\#\#\#}P < 0.001$ vs. AOH). Data are presented as mean ± SEM. (For interpretation of the references to color in this figure legend, the reader is referred to the Web version of this article.)

3.7. Acute ocular hypertension has a poor prognosis for intraocular pressure , and NAC and VX-765 significantly reduce IOPs in acute ocular hypertension eyes

To gain better insight on the IOP outcomes post-acute injury, and to ascertain the protective efficacy of NAC and VX-765 on TM

tissues in vivo, we monitored the IOP daily across all experimental rat groups (A-E) over one week. Results revealed that the AOH group experienced significant IOP increases from day 1 to day 7 compared to the control group (Fig. 7A). Intriguingly, after the first day of treatment with NAC or VX-765, there was a significant drop in IOP compared to the PBS-treated group (mean SD mmHg) ($p <$ 0.01) (group C). This IOP-lowering effect was sustained throughout the seven days for the NAC and VX-765 groups. IOP was gradually recovered to baseline levels for the observation period in the NAC and VX-765 groups (Fig. 7B). This data further supports the potential protective effect of NAC and VX-765 against elevated IOP.

4. Discussion

Acute glaucoma is a major cause of irreversible blindness worldwide characterized by a sudden and significant increase in IOP [42,43]. The combination of direct mechanical pressure and the excessive production of ROS due to elevated IOP is widely acknowledged as the primary factor underlying glaucoma-related injuries [29]. The TM plays a crucial role in maintaining the aqueous outflow pathway, rendering it a central player in the pathogenesis of glaucoma [43,44]. Currently, controlling IOP within a safe range is considered the primary therapeutic approach for managing acute glaucoma [45–47]. Unfortunately, there remains a dearth of effective and validated therapeutic strategies specifically targeting glaucomatous TM dysfunction, this underscores the need to explore novel targets and interventions to prevent and ameliorate the damages of acute glaucoma. Our study demonstrates the activation of NLRP3/caspase-1/IL-1β pyroptosis pathway in H_2O_2-exposed TM cells in vitro and in an AOH rodent model. By reducing ROS production or inhibiting caspase-1, we were able to prevent ROS-induced inflammation and pyroptosis in TM, both in vitro and in vivo. This suggests the potential of NAC/VX-765 as a promising pharmaceutical intervention for IOP reduction.

Pyroptosis, a form of non-apoptotic programmed cell death, has gained prominence in recent studies due to its crucial role in inflammation in various ocular diseases [12,14]. Specifically, NLRP3 activation, induced by infections like Aspergillus fumigatus infection in fungal keratitis or herpes simplex virus type 1(HSV-1) infection in viral keratitis, leads to pyroptosis [48,49]. High expression of NLRP3, caspase-1, and IL-1β are also found in patients with diabetic retinopathy [50,51] and other ocular diseases such

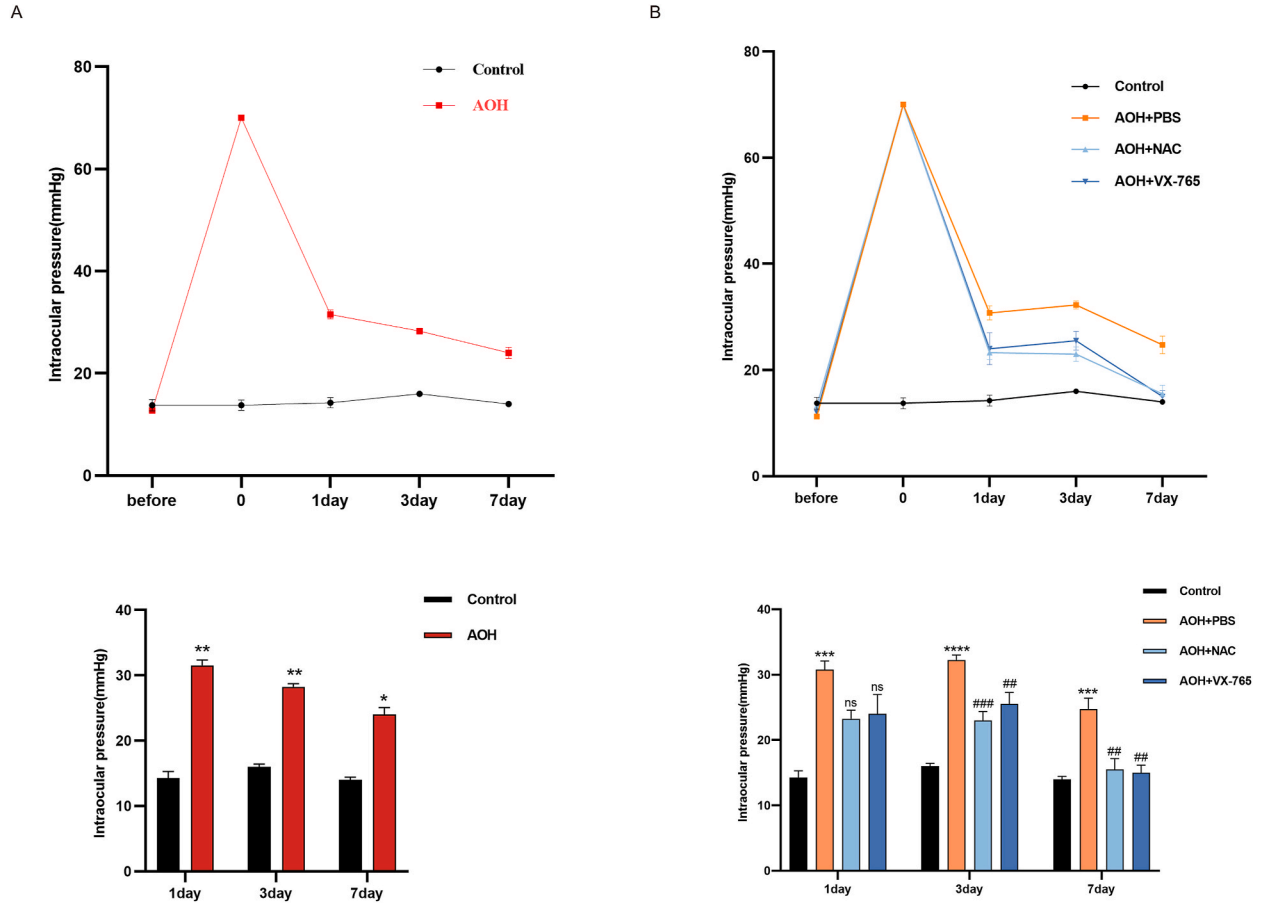

Fig. 7. Effect of AOH exposure and NAC or VX-765 treatment on IOP in rats. (7A) IOP of rats at 1, 3, and 7 days after AOH was significantly elevated compared to the control group. (7B). NAC and VX-765 treatment effectively ameliorated the prognosis of IOP elevation caused by AOH in vivo ($n \geq 4$). $^{*}P < 0.05$, $^{**}P < 0.01$, $^{***}P < 0.001$ vs. control, $^{\#\#}P < 0.01$, $^{\#\#\#}P < 0.001$ vs. AOH). Data are presented as mean ± SEM.

as uveitis and cataracts [52,53]. However, the exact role of pyroptosis in TM in glaucoma remains unclear. Notably, TM samples from glaucoma patients who had undergone trabeculectomy exhibited a significantly higher expression of NLRP3 and caspase 1 compared to the control group without associated ocular pathologies. The increased expressions imply an important role of pyroptosis in the progression of glaucoma.

Previous studies have underscored the importance of pyroptosis in the pathogenesis of acute glaucoma, primarily focusing on the death mechanisms of RGCs [15,28]. In a murine retinal ischemia/reperfusion (RIR) model, it was observed that microglia-induced pyroptosis contributed to RGC death, leading to vision loss [28]. Chi et al. suggests that targeted inhibition of caspase-8 down-regulated TLR4-mediated activation of NLRP1 and NLRP3, which significantly blocked the production of IL-1β and attenuated RGC death [54]. The TM, essential for AH drainage, is particularly susceptible to mitochondrial oxidative injury, which can lead to elevated IOP, a precursor of glaucoma [55]. Li et al. found that $PM_{2.5}$ exposure induced a significant elevation of ROS, and subsequently an increase in the expression of NLRP3, caspase-1, IL-1β, and GSDMD proteins in both HTM cells and TM of mice [20]. Similarly, in our study, we observed an activation of the classical pyroptosis pathway, NLRP3/caspase-1, in TM tissues from human glaucoma patients, rat acute glaucoma model, and H_2O_2-induced HTM cells.

H_2O_2 is commonly used for in vitro cellular oxidative damage models, such as TM cell injury [56,57]. The present study employed H_2O_2 to induce intracellular ROS, and further investigate the effects of pyroptosis in TM. Different concentrations (0 μM, 100 μM, 200 μM and 300 μM) of H_2O_2 were applied to the HTM cells. After 0 h, 6 h, 12 h, and 24 h, HTM cells viability was tested by CCK8. Cell viability significantly decreased after 300 μM of H_2O_2 for 6 h. Pyroptosis was tested by CCK8, RT-qPCR, ELISA, and WB after 200 μM of H_2O_2 for 0 h, 6 h, 12 h, and 24 h. Similar to the previous study, we found that pyroptosis was time- and concentration-dependent in H_2O_2 treatment [38]. Therefore, we chose 200 μM H_2O_2 for 12 h to establish an oxidative stress model to study pyroptosis in TM cells.

The NLRP3 inflammasome, a key regulatory factor of pyroptosis and inflammation, has been demonstrated to engage in glaucoma pathogenesis [20,28]. It activates the IL-1β-dependent inflammatory, leading to cell death in conditions marked by inflammation and stress [58]. Due to its capacity to respond to various stimuli, NLRP3 serves as a critical integrator of cellular stress. Research indicates that NLRP3 inflammasome can be activated by exogenous stimuli such as LPS and endogenous injury signals such as ATP, inducing ROS production, and subsequently caspase-1-dependent pyroptosis [13,59]. Specifically, when ROS overload is induced, the NLRP3 inflammasome activates, catalyzing the conversion of pro-caspase-1 to its active state [60–62]. Previous studies have demonstrated that oxidative stress caused by high intraocular pressure occurs in both the retina and the TM [63,64]. The TM is more vulnerable to oxidative damage due to its limited antioxidant defense [65]. We hypothesized that AOH may lead to excessive ROS accumulation in the AH, inducing TM pyroptosis. We confirmed this by demonstrating the effect of H_2O_2-induced ROS overload on TM pyroptosis in vitro. Additionally, AOH was further used to disrupt the REDOX balance of the intraocular outflow channel in vivo. We observed NLRP3/caspase-1/IL-1β related pyroptosis pathway in rat TM tissues after AOH, suggesting that AOH aggravates the inflammatory damage of TM.

NAC, a widely used antioxidant, possesses a robust capability to scavenge hydroxyl radicals and modulate inflammatory cascades. It has been extensively utilized in the treatment of corneal wounds, keratitis, conjunctivitis, and other ocular diseases [66,67]. On the other hand, VX-765 is an effective selective caspase-1 inhibitor with potent anti-inflammatory activity by inhibiting the release of inflammatory cytokines. In a mice diabetes model, VX-765 has been shown to ameliorate renal injury by modulating caspase-1-mediated pyroptosis and inflammation [68]. In this study, we further explored the effectiveness of these ROS/pyroptosis inhibitors both in vitro and in vivo. Consistent with previous studies, our results suggested that NAC (10 mM) or VX-765 (100 μM) pretreatment bolstered HTM cell survival following H_2O_2 exposure. Additionally, this pretreatment significantly reduced the levels of NLRP3, caspase-1, and IL-1β levels in HTM cells. Pivoting from these in vitro results, we employed NAC and VX-765 in a rat model of AOH. Compared with the control group, the mRNA levels of NLRP3, caspase-1, and IL-1β in TM tissues were significantly reduced after NAC and VX-765 treatment. These results highlight the potent anti-pyroptotic and anti-inflammatory effects of these compounds.

AOH is the most important characteristic of acute glaucoma, potentially causing damage from the back to the front of the eye [69,70]. While some experiments have demonstrated ultrastructural changes in TM following acute and chronic ocular hypertension [25,71–73], the ramifications of structural injuries to AH angle on intraocular pressure have been insufficiently investigated in current literature. Previously, we have demonstrated that the TM tissue underwent pyroptotic injury following AOH induction. The ensuing changes in IOP following TM injury are of paramount concern. Therefore, we monitored the level of IOP fluctuation for one week after ocular hypertension induction. Our results revealed that the high intraocular pressure group consistently exhibited higher levels of IOP throughout the week compared to their normal counterparts, indicating that acute ocular hypertension causes irreversible functional damage to the TM.

The pharmacological effects of NAC and VX-765 on IOP were further investigated. In our study, a single AH injection of NAC (4 μL, 20 mM) or VX-765(4 μL, 200 μM) effectively alleviated the elevated IOP over a span of one week. During this period, the IOP values in the drug-treated group remained consistently lower than in the control group. By the seventh day, the elevation of IOP was largely reversed. These findings further support the potential therapeutic efficacy of NAC and VX-765 in managing acute ocular hypertension in vivo. This study is the first to demonstrate the protective effects of NAC and VX-765 on the TM after AOH in rats, highlighting their significance for future applications in acute glaucoma therapy.

In our study, tissue sampling was conducted 2 h after the induction of ocular hypertension or after administering the drug intervention. Sun et al. have pointed out that a significant increase of oxygen free radicals was detected in the AH and TM of an AOH animal model as early as 0.5 h after acute ocular hypertension and this upward trend persisted for up to 72 h. These findings indicate potential damage in the TM caused by free radicals following acute ocular hypertension [74]. Pyroptosis is closely related to elevated levels of ROS, which frequently serves as a potent activator of NLRP3 [13,75]. In our experiments, a significant increase in key proteins of the classical pyroptosis pathway was detected in the TM tissues obtained at the set sampling time compared to the control group.

Furthermore, the result of the week-long IOP monitoring suggested sustained damage to the TM. Given these findings, future studies need to include multiple time points after acute ocular hypertension to further elucidate the impact of pyroptosis on TM damage.

There are several limitations to this study. The in vivo experiments using rats to reproduce glaucoma may not fully mimic the complex human scenario. In future studies, we will focus on the expression in human cells, increasing the duration of exposure of HTM cells to H_2O_2, to assess the potential adaptive response of TM cells to stress conditions and the regulation of cell death signals. Further research is also warranted to delve deeper into the exploration of human TM tissue and animal experiments. Meantime, the small TM sample size might provide difficulties and effects on the IHC staining study. The sample size will be further optimized in future studies. Next, while our data demonstrate the potential pathogenic role of the classical pyroptosis pathway NLRP3/caspase-1/IL-1β in TM, it is important to note that cell death is a complex process that encompasses multiple pathways and their crosstalk. Therefore, it is imperative to further investigate other cell death pathways in TM. Lastly, although the application of inhibitors (NAC and VX-765) has shown promise in protecting TM from pyroptosis, further verification is still required to determine their therapeutic efficacy.

Our study has demonstrated that the overproduction of ROS and elevated IOP triggers increased NLRP3/caspase-1 expression and production of IL-1β. These elements collectively drive IOP-induced TM pyroptosis. This perspective was further validated. NAC and VX-765 effectively attenuated ROS-induced caspase1-dependent pyroptosis and inflammation in TM both in vivo and in vitro. This further suggests that NAC and VX-765 provided protection to the TM by inhibition of ROS/NLRP3/caspase-1/il-1β-initiated pyroptosis, and the utilization may potentially serve as a promising strategy for the innovative treatment of acute glaucoma. More importantly, our study provides evidence that NAC and VX-765 effectively control persistent ocular hypertension after acute ocular hypertension injury in rats. These findings provide novel insights into the role of pyroptosis in injuries to the TM caused by ROS and AOH.

Funding

1. SBGJ2018083 (Henan Medical Science Foundation of China) to Qian Liu.
2. No.21JCQN005 (Basic Research Project of Henan Provincial Eye Hospital) to Qian Liu.
3. 222300420196 (Natural Science Foundation of Henan Province, China) to Qian Liu.
4. 23456 Talent Development (Henan Provincial People's Hospital, China) to Qian Liu.

This work was also supported, in part, by the National Natural Science Foundation of China, China (no. U1404812 to Qian Liu).

Ethics and consent section

Informed consent was obtained from all participants and/or their guardians.

Data availability statement

The authors confirm that the data supporting the findings of this study are available within the article and its supplementary materials.

CRediT authorship contribution statement

Xiaomei Feng: Writing – review & editing, Writing – original draft, Validation, Methodology, Data curation. **Zhao Chen:** Writing – review & editing. **Wenjun Cheng:** Writing – review & editing. **Changgeng Liu:** Writing – review & editing. **Qian Liu:** Writing – review & editing, Supervision.

Declaration of competing interest

The authors declare that they have no known competing financial interests or personal relationships that could have appeared to influence the work reported in this paper.

Acknowledgments

We sincerely thank the Eye Bank of Henan Eye Hospital for their valuable contributions, which greatly facilitated the successful completion of this study. We also express our heartfelt appreciation to the dedicated participants whose voluntary involvement was pivotal to our research.

References

[1] R.N. Weinreb, T. Aung, F.A. Medeiros, R.N. Weinreb, T. Aung, F.A. Medeiros, The pathophysiology and treatment of glaucoma: a review, JAMA 311 (18) (2014) 1901–1911.
[2] W.-K. Ju, G.A. Perkins, K.-Y. Kim, T. Bastola, W.-Y. Choi, S.-H. Choi, W.-K. Ju, G.A. Perkins, K.-Y. Kim, T. Bastola, W.-Y. Choi, S.-H. Choi, Glaucomatous optic neuropathy: mitochondrial dynamics, dysfunction and protection in retinal ganglion cells, Prog. Retin. Eye Res. 95 (2023) 101136.

[3] A. Hakim, B. Guido, L. Narsineni, D.-W. Chen, M. Foldvari, A. Hakim, B. Guido, L. Narsineni, D.-W. Chen, M. Foldvari, Gene therapy strategies for glaucoma from IOP reduction to retinal neuroprotection: progress towards non-viral systems, Adv. Drug Deliv. Rev. 196 (2023) 114781.

[4] O.-Y. Tektas, E. Lütjen-Drecoll, O.-Y. Tektas, E. Lütjen-Drecoll, Structural changes of the trabecular meshwork in different kinds of glaucoma, Exp. Eye Res. 88 (4) (2009) 769–775.

[5] D.O. Schachtschabel, E.A. Binninger, J.W. Rohen, D.O. Schachtschabel, E.A. Binninger, J.W. Rohen, In vitro cultures of trabecular meshwork cells of the human eye as a model system for the study of cellular aging, Arch. Gerontol. Geriatr. 9 (3) (1989) 251–262.

[6] J. Alvarado, C. Murphy, R. Juster, J. Alvarado, C. Murphy, R. Juster, Trabecular meshwork cellularity in primary open-angle glaucoma and nonglaucomatous normals, Ophthalmology 91 (6) (1984) 564–579.

[7] M.M. Rodrigues, G.L. Spaeth, E. Sivalingam, S. Weinreb, M.M. Rodrigues, G.L. Spaeth, E. Sivalingam, S. Weinreb, Histopathology of 150 trabeculectomy specimens in glaucoma, Trans. Ophthalmol. Soc. U. K. 96 (2) (1976) 245–255.

[8] W. Zhu, O.W. Gramlich, L. Laboissonniere, A. Jain, V.C. Sheffield, J.M. Trimarchi, B.A. Tucker, M.H. Kuehn, W. Zhu, O.W. Gramlich, L. Laboissonniere, A. Jain, V.C. Sheffield, J.M. Trimarchi, B.A. Tucker, M.H. Kuehn, Transplantation of iPSC-derived TM cells rescues glaucoma phenotypes in vivo, Proc. Natl. Acad. Sci. U. S. A. 113 (25) (2016) E3492–E3500.

[9] J.Y. Bermudez, M. Montecchi-Palmer, W. Mao, A.F. Clark, J.Y. Bermudez, M. Montecchi-Palmer, W. Mao, A.F. Clark, Cross-linked actin networks (CLANs) in glaucoma, Exp. Eye Res. 159 (2017) 16–22.

[10] J.A. Last, T. Pan, Y. Ding, C.M. Reilly, K. Keller, T.S. Acott, M.P. Fautsch, C.J. Murphy, P. Russell, J.A. Last, T. Pan, Y. Ding, C.M. Reilly, K. Keller, T.S. Acott, M. P. Fautsch, C.J. Murphy, P. Russell, Elastic modulus determination of normal and glaucomatous human trabecular meshwork, Invest. Ophthalmol. Vis. Sci. 52 (5) (2011) 2147–2152.

[11] S.-K. Hsu, C.-Y. Li, I.L. Lin, W.-J. Syue, Y.-F. Chen, K.-C. Cheng, Y.-N. Teng, Y.-H. Lin, C.-H. Yen, C.-C. Chiu, S.-K. Hsu, C.-Y. Li, I.L. Lin, W.-J. Syue, Y.-F. Chen, K.-C. Cheng, Y.-N. Teng, Y.-H. Lin, C.-H. Yen, C.-C. Chiu, Inflammation-related pyroptosis, a novel programmed cell death pathway, and its crosstalk with immune therapy in cancer treatment, Theranostics 11 (18) (2021) 8813–8835.

[12] Y. Zhang, Y. Jiao, X. Li, S. Gao, N. Zhou, J. Duan, M. Zhang, Y. Zhang, Y. Jiao, X. Li, S. Gao, N. Zhou, J. Duan, M. Zhang, Pyroptosis: a new insight into eye disease therapy, Front. Pharmacol. 12 (2021).

[13] Z. Qiu, Y. He, H. Ming, S. Lei, Y. Leng, Z.-Y. Xia, Z. Qiu, Y. He, H. Ming, S. Lei, Y. Leng, Z.-Y. Xia, Lipopolysaccharide (LPS) aggravates high glucose- and hypoxia/reoxygenation-induced injury through activating ROS-dependent NLRP3 inflammasome-mediated pyroptosis in H9C2 cardiomyocytes, J. Diabetes Res. 2019 (2019) 8151836.

[14] M. Chen, R. Rong, X. Xia, M. Chen, R. Rong, X. Xia, Spotlight on pyroptosis: role in pathogenesis and therapeutic potential of ocular diseases, J. Neuroinflammation 19 (1) (2022) 183.

[15] C. Meng, C. Gu, S. He, T. Su, T. Lhamo, D. Draga, Q. Qiu, C. Meng, C. Gu, S. He, T. Su, T. Lhamo, D. Draga, Q. Qiu, Pyroptosis in the retinal neurovascular unit: new insights into diabetic retinopathy, Front. Immunol. 12 (2021) 763092.

[16] M. Yang, K.-F. So, W.C. Lam, A.C.Y. Lo, M. Yang, K.-F. So, W.C. Lam, A.C.Y. Lo, Novel programmed cell death as therapeutic targets in age-related macular degeneration? Int. J. Mol. Sci. 21 (19) (2020).

[17] M. Almasieh, A.M. Wilson, B. Morquette, J.L. Cueva Vargas, A. Di Polo, M. Almasieh, A.M. Wilson, B. Morquette, J.L. Cueva Vargas, A. Di Polo, The molecular basis of retinal ganglion cell death in glaucoma, Prog. Retin. Eye Res. 31 (2) (2012) 152–181.

[18] A. Pronin, D. Pham, W. An, G. Dvoriantchikova, G. Reshetnikova, J. Qiao, Z. Kozhekbaeva, A.E. Reiser, V.Z. Slepak, V.I. Shestopalov, A. Pronin, D. Pham, W. An, G. Dvoriantchikova, G. Reshetnikova, J. Qiao, Z. Kozhekbaeva, A.E. Reiser, V.Z. Slepak, V.I. Shestopalov, Inflammasome activation induces pyroptosis in the retina exposed to ocular hypertension injury, Front. Mol. Neurosci. 12 (2019) 36.

[19] Q. Zheng, Y. Ren, P.S. Reinach, Y. She, B. Xiao, S. Hua, J. Qu, W. Chen, Q. Zheng, Y. Ren, P.S. Reinach, Y. She, B. Xiao, S. Hua, J. Qu, W. Chen, Reactive oxygen species activated NLRP3 inflammasomes prime environment-induced murine dry eye, Exp. Eye Res. 125 (2014) 1–8.

[20] L. Li, C. Xing, J. Zhou, L. Niu, B. Luo, M. Song, J. Niu, Y. Ruan, X. Sun, Y. Lei, L. Li, C. Xing, J. Zhou, L. Niu, B. Luo, M. Song, J. Niu, Y. Ruan, X. Sun, Y. Lei, Airborne particulate matter (PM(2.5)) triggers ocular hypertension and glaucoma through pyroptosis, Part. Fibre Toxicol. 18 (1) (2021) 10.

[21] E.F. Baser, G. Seymenoglu, H. Mayali, E.F. Baser, G. Seymenoglu, H. Mayali, Trabeculectomy for advanced glaucoma, Int. Ophthalmol. 31 (6) (2011) 439–446.

[22] A.J. King, J. Hudson, G. Fernie, A. Kernohan, A. Azuara-Blanco, J. Burr, T. Homer, H. Shabaninejad, J.M. Sparrow, D. Garway-Heath, , et al.A.J. King, J. Hudson, G. Fernie, A. Kernohan, A. Azuara-Blanco, J. Burr, T. Homer, H. Shabaninejad, J.M. Sparrow, D. Garway-Heath, et al., Primary trabeculectomy for advanced glaucoma: pragmatic multicentre randomised controlled trial (TAGS), BMJ 373 (2021) n1014.

[23] E. Moisseiev, E. Zunz, R. Tzur, S. Kurtz, G. Shemesh, E. Moisseiev, E. Zunz, R. Tzur, S. Kurtz, G. Shemesh, Standard trabeculectomy and ex-PRESS miniature glaucoma shunt: a comparative study and literature review, J. Glaucoma 24 (6) (2015) 410–416.

[24] R. Sihota, A. Goyal, J. Kaur, V. Gupta, T.C. Nag, R. Sihota, A. Goyal, J. Kaur, V. Gupta, T.C. Nag, Scanning electron microscopy of the trabecular meshwork: understanding the pathogenesis of primary angle closure glaucoma, Indian J. Ophthalmol. 60 (3) (2012) 183–188.

[25] X. Li, Z. Zhang, L. Ye, J. Meng, Z. Zhao, Z. Liu, J. Hu, X. Li, Z. Zhang, L. Ye, J. Meng, Z. Zhao, Z. Liu, J. Hu, Acute ocular hypertension disrupts barrier integrity and pump function in rat corneal endothelial cells, Sci. Rep. 7 (1) (2017) 6951.

[26] T. Ramaesh, K. Ramaesh, S.C. Riley, J.D. West, B. Dhillon, T. Ramaesh, K. Ramaesh, S.C. Riley, J.D. West, B. Dhillon, Effects of N-acetylcysteine on matrix metalloproteinase-9 secretion and cell migration of human corneal epithelial cells, Eye 26 (8) (2012) 1138–1144.

[27] Y. Sun, T. Liu, Y. Sun, T. Liu, Acute ocular hypertension induced pyroptosis in rat retinal ganglion cells and protective effect of inhibiting Caspase-1 in rat model, Journal of Army Medical University 44 (8) (2022) 789–796.

[28] H. Chen, Y. Deng, X. Gan, Y. Li, W. Huang, L. Lu, L. Wei, L. Su, J. Luo, B. Zou, , et al.H. Chen, Y. Deng, X. Gan, Y. Li, W. Huang, L. Lu, L. Wei, L. Su, J. Luo, B. Zou, et al., NLRP12 collaborates with NLRP3 and NLRC4 to promote pyroptosis inducing ganglion cell death of acute glaucoma, Mol. Neurodegener. 15 (1) (2020) 26.

[29] F. Yao, J. Peng, E. Zhang, D. Ji, Z. Gao, Y. Tang, X. Yao, X. Xia, F. Yao, J. Peng, E. Zhang, D. Ji, Z. Gao, Y. Tang, X. Yao, X. Xia, Pathologically high intraocular pressure disturbs normal iron homeostasis and leads to retinal ganglion cell ferroptosis in glaucoma, Cell Death Differ. 30 (1) (2023) 69–81.

[30] Q. Liu, K. Wu, X. Qiu, Y. Yang, X. Lin, M. Yu, Q. Liu, K. Wu, X. Qiu, Y. Yang, X. Lin, M. Yu, siRNA silencing of gene expression in trabecular meshwork: RhoA siRNA reduces IOP in mice, Curr. Mol. Med. 12 (8) (2012) 1015–1027.

[31] B. Luo, B. Li, W. Wang, X. Liu, Y. Xia, C. Zhang, M. Zhang, Y. Zhang, F. An, B. Luo, B. Li, W. Wang, X. Liu, Y. Xia, C. Zhang, M. Zhang, Y. Zhang, F. An, NLRP3 gene silencing ameliorates diabetic cardiomyopathy in a type 2 diabetes rat model, PLoS One 9 (8) (2014) e104771.

[32] Z. He, Y. Ma, S. Yang, S. Zhang, S. Liu, J. Xiao, Y. Wang, W. Wang, H. Yang, S. Li, , et al.Z. He, Y. Ma, S. Yang, S. Zhang, S. Liu, J. Xiao, Y. Wang, W. Wang, H. Yang, S. Li, et al., Gut microbiota-derived ursodeoxycholic acid from neonatal dairy calves improves intestinal homeostasis and colitis to attenuate extended-spectrum β-lactamase-producing enteroaggregative Escherichia coli infection, Microbiome 10 (1) (2022) 79.

[33] X. Wu, H. Zhang, W. Qi, Y. Zhang, J. Li, Z. Li, Y. Lin, X. Bai, X. Liu, X. Chen, , et al.X. Wu, H. Zhang, W. Qi, Y. Zhang, J. Li, Z. Li, Y. Lin, X. Bai, X. Liu, X. Chen, et al., Nicotine promotes atherosclerosis via ROS-NLRP3-mediated endothelial cell pyroptosis, Cell Death Dis. 9 (2) (2018) 171.

[34] S.P.T. Yiu, C. Zerbe, D. Vanderwall, E.L. Huttlin, M.P. Weekes, B.E. Gewurz, S.P.T. Yiu, C. Zerbe, D. Vanderwall, E.L. Huttlin, M.P. Weekes, B.E. Gewurz, An Epstein-Barr virus protein interaction map reveals NLRP3 inflammasome evasion via MAVS UFMylation, Mol. Cell 83 (13) (2023).

[35] X.-R. Huang, Y. Zhou, W. Kong, R.W. Knighton, X.-R. Huang, Y. Zhou, W. Kong, R.W. Knighton, Reflectance decreases before thickness changes in the retinal nerve fiber layer in glaucomatous retinas, Invest. Ophthalmol. Vis. Sci. 52 (9) (2011) 6737–6742.

[36] W.-H. Wang, J.C. Millar, I.-H. Pang, M.B. Wax, A.F. Clark, W.-H. Wang, J.C. Millar, I.-H. Pang, M.B. Wax, A.F. Clark, Noninvasive measurement of rodent intraocular pressure with a rebound tonometer, Invest. Ophthalmol. Vis. Sci. 46 (12) (2005) 4617–4621.

[37] A. Hosseini, F.A. Lattanzio, P.B. Williams, D. Tibbs, S.S. Samudre, R.C. Allen, A. Hosseini, F.A. Lattanzio, P.B. Williams, D. Tibbs, S.S. Samudre, R.C. Allen, Chronic topical administration of WIN-55-212-2 maintains a reduction in IOP in a rat glaucoma model without adverse effects, Exp. Eye Res. 82 (5) (2006) 753–759.

[38] X. Jin, H. Jin, Y. Shi, Y. Guo, H. Zhang, X. Jin, H. Jin, Y. Shi, Y. Guo, H. Zhang, Pyroptosis, a novel mechanism implicated in cataracts, Mol. Med. Rep. 18 (2) (2018) 2277–2285.

[39] W.-H. Xie, J. Ding, X.-X. Xie, X.-H. Yang, X.-F. Wu, Z.-X. Chen, Q.-L. Guo, W.-Y. Gao, X.-Z. Wang, D. Li, W.-H. Xie, J. Ding, X.-X. Xie, X.-H. Yang, X.-F. Wu, Z.-X. Chen, Q.-L. Guo, W.-Y. Gao, X.-Z. Wang, D. Li, Hepatitis B virus X protein promotes liver cell pyroptosis under oxidative stress through NLRP3 inflammasome activation, Inflamm. Res. 69 (7) (2020) 683–696.

[40] Y. Wang, H. Zhou, X. Liu, Y. Han, S. Pan, Y. Wang, Y. Wang, H. Zhou, X. Liu, Y. Han, S. Pan, Y. Wang, MiR-181a inhibits human trabecular meshwork cell apoptosis induced by H_2O_2 through the suppression of NF-κB and JNK pathways, Adv. Clin. Exp. Med. 27 (5) (2018) 577–582.

[41] M.-C. Xu, X.-F. Gao, C. Ruan, Z.-R. Ge, J.-D. Lu, J.-J. Zhang, Y. Zhang, L. Wang, H.-M. Shi, M.-C. Xu, X.-F. Gao, C. Ruan, Z.-R. Ge, J.-D. Lu, J.-J. Zhang, Y. Zhang, L. Wang, H.-M. Shi, miR-103 regulates oxidative stress by targeting the BCL2/adenovirus E1B 19 kDa interacting protein 3 in HUVECs, Oxid. Med. Cell. Longev. 2015 (2015) 489647.

[42] W. Chi, H. Chen, F. Li, Y. Zhu, W. Yin, Y. Zhuo, W. Chi, H. Chen, F. Li, Y. Zhu, W. Yin, Y. Zhuo, HMGB1 promotes the activation of NLRP3 and caspase-8 inflammasomes via NF-kappaB pathway in acute glaucoma, J. Neuroinflammation 12 (2015) 137.

[43] S. Tabak, S. Schreiber-Avissar, E. Beit-Yannai, S. Tabak, S. Schreiber-Avissar, E. Beit-Yannai, Crosstalk between MicroRNA and oxidative stress in primary open-angle glaucoma, Int. J. Mol. Sci. 22 (5) (2021).

[44] J. Buffault, A. Labbé, P. Hamard, F. Brignole-Baudouin, C. Baudouin, J. Buffault, A. Labbé, P. Hamard, F. Brignole-Baudouin, C. Baudouin, The trabecular meshwork: structure, function and clinical implications. A review of the literature, J. Fr. Ophtalmol. 43 (7) (2020) e217–e230.

[45] P.C. VanVeldhuisen, F. Ederer, D.E. Gaasterland, E.K. Sullivan, A. Beck, B.E. Prum, M.N. Cyrlin, H. Weiss, P.C. VanVeldhuisen, F. Ederer, D.E. Gaasterland, E. K. Sullivan, A. Beck, B.E. Prum, M.N. Cyrlin, H. Weiss, The Advanced Glaucoma Intervention Study (AGIS): 7. The relationship between control of intraocular pressure and visual field deterioration.The AGIS Investigators, Am. J. Ophthalmol. 130 (4) (2000) 429–440.

[46] D.R. Anderson, S.M. Drance, M. Schulzer, D.R. Anderson, S.M. Drance, M. Schulzer, Natural history of normal-tension glaucoma, Ophthalmology 108 (2) (2001) 247–253.

[47] B.L. Lee, M.R. Wilson, B.L. Lee, M.R. Wilson, Ocular hypertension treatment study (OHTS) commentary, Curr. Opin. Ophthalmol. 14 (2) (2003) 74–77.

[48] S.-L. Wang, G. Zhao, W. Zhu, X.-M. Dong, T. Liu, Y.-Y. Li, W.-G. Song, Y.-Q. Wang, S.-L. Wang, G. Zhao, W. Zhu, X.-M. Dong, T. Liu, Y.-Y. Li, W.-G. Song, Y.-Q. Wang, Herpes simplex virus-1 infection or Simian virus 40-mediated immortalization of corneal cells causes permanent translocation of NLRP3 to the nuclei, Int. J. Ophthalmol. 8 (1) (2015) 46–51.

[49] W. Zhao, H. Yang, L. Lyu, J. Zhang, Q. Xu, N. Jiang, G. Liu, L. Wang, H. Yan, C. Che, W. Zhao, H. Yang, L. Lyu, J. Zhang, Q. Xu, N. Jiang, G. Liu, L. Wang, H. Yan, C. Che, GSDMD, an executor of pyroptosis, is involved in IL-1β secretion in Aspergillus fumigatus keratitis, Exp. Eye Res. 202 (2021) 108375.

[50] S. Loukovaara, N. Piippo, K. Kinnunen, M. Hytti, K. Kaarniranta, A. Kauppinen, S. Loukovaara, N. Piippo, K. Kinnunen, M. Hytti, K. Kaarniranta, A. Kauppinen, NLRP3 inflammasome activation is associated with proliferative diabetic retinopathy, Acta Ophthalmol. 95 (8) (2017) 803–808.

[51] Y. Zhang, X. Lv, Z. Hu, X. Ye, X. Zheng, Y. Ding, P. Xie, Q. Liu, Y. Zhang, X. Lv, Z. Hu, X. Ye, X. Zheng, Y. Ding, P. Xie, Q. Liu, Protection of Mcc950 against high-glucose-induced human retinal endothelial cell dysfunction, Cell Death Dis. 8 (7) (2017) e2941.

[52] E. Ugurel, E. Erdag, C.I. Kucukali, A. Olcay, E. Sanli, E. Akbayir, M. Kurtuncu, T. Gunduz, V. Yilmaz, E. Tuzun, , et al.E. Ugurel, E. Erdag, C.I. Kucukali, A. Olcay, E. Sanli, E. Akbayir, M. Kurtuncu, T. Gunduz, V. Yilmaz, E. Tuzun, et al., Enhanced NLRP3 and DEFA1B expression during the active stage of parenchymal neuro-behçet's disease, In Vivo 33 (5) (2019) 1493–1497.

[53] Y. Sun, X. Rong, D. Li, Y. Jiang, Y. Lu, Y. Ji, Y. Sun, X. Rong, D. Li, Y. Jiang, Y. Lu, Y. Ji, Down-regulation of CRTAC1 attenuates UVB-induced pyroptosis in HLECs through inhibiting ROS production, Biochem. Biophys. Res. Commun. 532 (1) (2020) 159–165.

[54] W. Chi, F. Li, H. Chen, Y. Wang, Y. Zhu, X. Yang, J. Zhu, F. Wu, H. Ouyang, J. Ge, , et al.W. Chi, F. Li, H. Chen, Y. Wang, Y. Zhu, X. Yang, J. Zhu, F. Wu, H. Ouyang, J. Ge, et al., Caspase-8 promotes NLRP1/NLRP3 inflammasome activation and IL-1β production in acute glaucoma, Proc. Natl. Acad. Sci. U. S. A. 111 (30) (2014) 11181–11186.

[55] S.C. Saccà, A.M. Roszkowska, A. Izzotti, S.C. Saccà, A.M. Roszkowska, A. Izzotti, Environmental light and endogenous antioxidants as the main determinants of non-cancer ocular diseases, Mutat. Res. 752 (2) (2013) 153–171.

[56] E.J. Snider, B.A. Hardie, Y. Li, K. Gao, F. Splaine, R.K. Kim, R.T. Vannatta, A.T. Read, C.R. Ethier, E.J. Snider, B.A. Hardie, Y. Li, K. Gao, F. Splaine, R.K. Kim, R. T. Vannatta, A.T. Read, C.R. Ethier, A porcine organ-culture glaucoma model mimicking trabecular meshwork damage using oxidative stress, Invest. Ophthalmol. Vis. Sci. 62 (3) (2021) 18.

[57] S. Vernazza, M. Passalacqua, S. Tirendi, B. Marengo, C. Domenicotti, D. Sbardella, F. Oddone, A.M. Bassi, S. Vernazza, M. Passalacqua, S. Tirendi, B. Marengo, C. Domenicotti, D. Sbardella, F. Oddone, A.M. Bassi, Citicoline eye drops protect trabecular meshwork cells from oxidative stress injury in a 3D in vitro glaucoma model, Int. J. Mol. Sci. 23 (19) (2022).

[58] C.L. Evavold, J.C. Kagan, C.L. Evavold, J.C. Kagan, Inflammasomes: threat-assessment organelles of the innate immune system, Immunity 51 (4) (2019) 609–624.

[59] Y. Jin, H. Li, G. Xie, S. Chen, S. Wu, X. Fang, Y. Jin, H. Li, G. Xie, S. Chen, S. Wu, X. Fang, Sevoflurane combined with ATP activates caspase-1 and triggers caspase-1-dependent pyroptosis in murine J774 macrophages, Inflammation 36 (2) (2013) 330–336.

[60] B. Bai, Y. Yang, Q. Wang, M. Li, C. Tian, Y. Liu, L.H.H. Aung, P.-F. Li, T. Yu, X.-M. Chu, B. Bai, Y. Yang, Q. Wang, M. Li, C. Tian, Y. Liu, L.H.H. Aung, P.-F. Li, T. Yu, X.-M. Chu, NLRP3 inflammasome in endothelial dysfunction, Cell Death Dis. 11 (9) (2020) 776.

[61] S.M. Man, T.-D. Kanneganti, S.M. Man, T.-D. Kanneganti, Regulation of inflammasome activation, Immunol. Rev. 265 (1) (2015).

[62] L. Minutoli, D. Puzzolo, M. Rinaldi, N. Irrera, H. Marini, V. Arcoraci, A. Bitto, G. Crea, A. Pisani, F. Squadrito, , et al.L. Minutoli, D. Puzzolo, M. Rinaldi, N. Irrera, H. Marini, V. Arcoraci, A. Bitto, G. Crea, A. Pisani, F. Squadrito, et al., ROS-mediated NLRP3 inflammasome activation in brain, heart, kidney, and testis ischemia/reperfusion injury, Oxid. Med. Cell. Longev. 2016 (2016) 2183026.

[63] M.C. Moreno, J. Campanelli, P. Sande, D.A. Sánez, M.I. Keller Sarmiento, R.E. Rosenstein, M.C. Moreno, J. Campanelli, P. Sande, D.A. Sánez, M.I. Keller Sarmiento, R.E. Rosenstein, Retinal oxidative stress induced by high intraocular pressure, Free Radic. Biol. Med. 37 (6) (2004) 803–812.

[64] J. Zhao, S. Wang, W. Zhong, B. Yang, L. Sun, Y. Zheng, J. Zhao, S. Wang, W. Zhong, B. Yang, L. Sun, Y. Zheng, Oxidative stress in the trabecular meshwork, Int. J. Mol. Med. 38 (4) (2016) (Review).

[65] S.C. Saccà, C.A. Cutolo, D. Ferrari, P. Corazza, C.E. Traverso, S.C. Saccà, C.A. Cutolo, D. Ferrari, P. Corazza, C.E. Traverso, The eye, oxidative damage and polyunsaturated fatty acids, Nutrients 10 (6) (2018).

[66] M. Halasi, M. Wang, T.S. Chavan, V. Gaponenko, N. Hay, A.L. Gartel, M. Halasi, M. Wang, T.S. Chavan, V. Gaponenko, N. Hay, A.L. Gartel, ROS inhibitor N-acetyl-L-cysteine antagonizes the activity of proteasome inhibitors, Biochem. J. 454 (2) (2013) 201–208.

[67] Y. Eghtedari, L.J. Oh, N.D. Girolamo, S.L. Watson, Y. Eghtedari, L.J. Oh, N.D. Girolamo, S.L. Watson, The role of topical N-acetylcysteine in ocular therapeutics, Surv. Ophthalmol. 67 (2) (2022) 608–622.

[68] H. Lyu, H. Ni, J. Huang, G. Yu, Z. Zhang, Q. Zhang, H. Lyu, H. Ni, J. Huang, G. Yu, Z. Zhang, Q. Zhang, VX-765 prevents intestinal ischemia-reperfusion injury by inhibiting NLRP3 inflammasome, Tissue Cell 75 (2022) 101718.

[69] X. Wang, J. Su, J. Ding, S. Han, W. Ma, H. Luo, G. Hughes, Z. Meng, Y. Yin, Y. Wang, , et al.X. Wang, J. Su, J. Ding, S. Han, W. Ma, H. Luo, G. Hughes, Z. Meng, Y. Yin, Y. Wang, et al., α-Aminoadipic acid protects against retinal disruption through attenuating Müller cell gliosis in a rat model of acute ocular hypertension, Drug Des. Dev. Ther. 10 (2016) 3449–3457.

[70] D. Ye, Y. Xu, Y. Shi, M. Fan, P. Lu, X. Bai, Y. Feng, C. Hu, K. Cui, X. Tang, , et al.D. Ye, Y. Xu, Y. Shi, M. Fan, P. Lu, X. Bai, Y. Feng, C. Hu, K. Cui, X. Tang, et al., Anti-PANoptosis is involved in neuroprotective effects of melatonin in acute ocular hypertension model, J. Pineal Res. 73 (4) (2022) e12828.

[71] R. Sihota, N.C. Lakshmaiah, K.B. Walia, S. Sharma, J. Pailoor, H.C. Agarwal, R. Sihota, N.C. Lakshmaiah, K.B. Walia, S. Sharma, J. Pailoor, H.C. Agarwal, The trabecular meshwork in acute and chronic angle closure glaucoma, Indian J. Ophthalmol. 49 (4) (2001) 255–259.

[72] R. Du, C. Xin, J. Xu, J. Hu, H. Wang, N. Wang, M. Johnstone, R. Du, C. Xin, J. Xu, J. Hu, H. Wang, N. Wang, M. Johnstone, Pulsatile trabecular meshwork motion: an indicator of intraocular pressure control in primary open-angle glaucoma, J. Clin. Med. 11 (10) (2022).

[73] B.M. Kerman, R.E. Christensen, R.Y. Foos, B.M. Kerman, R.E. Christensen, R.Y. Foos, Angle-closure glaucoma: a clinicopathologic correlation, Am. J. Ophthalmol. 76 (6) (1973) 887–895.
[74] W. Sun, Q. Meng, L. Yanyan, W. Sun, Q. Meng, L. Yanyan, The changes on free radical and catalase in ocular tissue of rabbits undergoing acute hypertenson status, Chinese Journal of Experimental Ophthalmology (2) (2001) 104–106.
[75] N. Kelley, D. Jeltema, Y. Duan, Y. He, N. Kelley, D. Jeltema, Y. Duan, Y. He, The NLRP3 inflammasome: an overview of mechanisms of activation and regulation, Int. J. Mol. Sci. 20 (13) (2019).